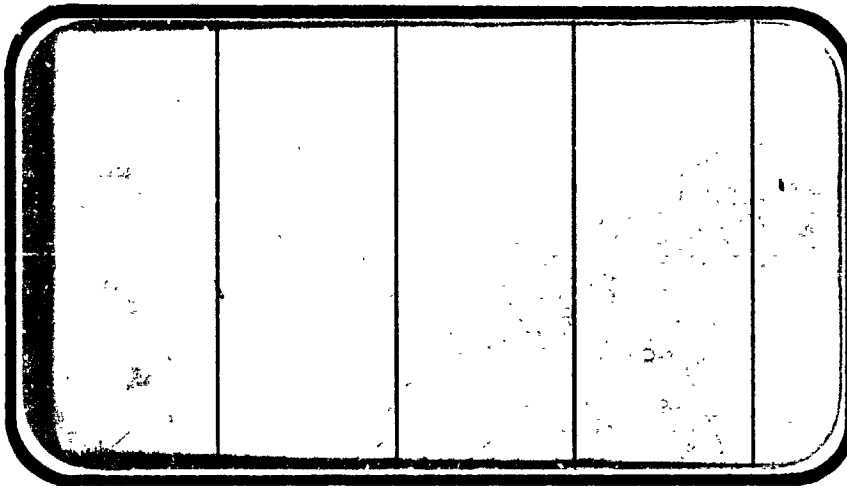


NATIONAL AERONAUTICS AND SPACE ADMINISTRATION

(NASA-CR-144618) RESULTS OF PHASE CHANGE
PAINT TESTS OF 0.04C SCALE 50% FOPEBCLY
MODELS (82-0) OF THE SPACE SHUTTLE CREITER
IN THE AEDC VKI B HYPERSONIC WIND TUNNEL
(OH75) (Chrysler Corp.) 32 p HC \$4.00

N76-23345

G3/18 Uncias
40662



SPACE SHUTTLE

AEROTHERMODYNAMIC DATA REPORT

JOHNSON SPACE CENTER

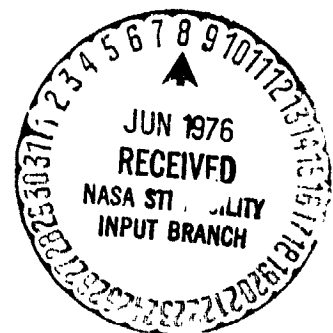
HOUSTON, TEXAS

DATA Management services

SPACE DIVISION



**CHRYSLER
CORPORATION**



April, 1976

DMS-DR-2303
NASA CR-144,618

RESULTS OF PHASE CHANGE PAINT TESTS OF
0.040 SCALE 50% FOREBODY MODELS (82-0)
OF THE SPACE SHUTTLE ORBITER IN THE
AEDC VKI B HYPERSONIC WIND TUNNEL (OH75)

by

W. H. Dye
Rockwell International Space Division

Prepared Under Contract No. NAS9-13247

by

Data Management Services
Chrysler Corporation Space Division
New Orleans, La. 70189

for

Engineering Analysis Division
Johnson Space Center
National Aeronautics and Space Administration
Houston, Texas

WIND TUNNEL TEST SPECIFICS:

Test Number: AEDC V41B - E3A
NASA Series Number: OH75
Model Number: 82-0
Test Date: September 1, 1975
Occupancy Hours: 8

FACILITY COORDINATOR:

L. L. Trimmer
VKF - SH
ARO, Inc.
Arnold Air Force Station,
Tennessee 37389

Phone: (615) 455-2611 x7377

DATA ANALYSIS ENGINEERS:

C. W. Craig and R. J. Curtis
Rockwell International
Space Division
12214 Lakewood Blvd.
Mail Code AC78
Downey, CA 90241

Phone: (213) 922-3076

PROJECT ENGINEERS:

W. H. Dye
Mail Code AC07
Rockwell International
Space Division
12214 Lakewood Blvd.
Downey, CA 90241

Phone: (213) 922-5005

L. Carter
VKF - SH
ARO, Inc.
Arnold Air Force Station,
Tennessee 37389

Phone: (615) 455-2611 x7377

DATA MANAGEMENT SERVICES:

Prepared by: Liaison -- D. A. Sarver
Operations--Maurice Moser, Jr.

Reviewed by: G. G. McDonald

Approved: J. L. Glynn
J. L. Glynn, Manager
Data Operations

Concurrence: N. D. Kemp
N. D. Kemp, Manager
Data Management Services

Chrysler Corporation Space Division assumes no responsibility for the data presented other than display characteristics.

RESULTS OF PHASE CHANGE PAINT TESTS OF
0.040 SCALE 50% FOREBODY MODELS (82-0)
OF THE SPACE SHUTTLE ORBITER IN THE
AEDC VKI B HYPERSONIC WIND TUNNEL (OH75)

by

W. H. Dye
Rockwell International Space Division

ABSTRACT

This report presents post-test information and data from phase change paint, aerodynamic heating wind tunnel tests of a Rockwell International Space Shuttle Orbiter forebody model. These tests were conducted in the Arnold Engineering and Development Center von Karman Facility Tunnel B Hypersonic Wind Tunnel.

The purpose of these tests was to determine the effect of simulated orbiter protuberances and penetrations (including RCS nozzles) on aerodynamic heating rates during simulated entry conditions.

TABLE OF CONTENTS

| | Page |
|---|------|
| ABSTRACT | iii |
| INDEX OF FIGURES | 2 |
| NOMENCLATURE | 4 |
| INTRODUCTION | 7 |
| CONFIGURATIONS INVESTIGATED | 8 |
| TEST FACILITY DESCRIPTION | 9 |
| TEST PROCEDURE | 10 |
| DATA REDUCTION | 12 |
| RESULTS AND DISCUSSION | 14 |
| REFERENCES | 16 |
| TABLES | |
| I. MODEL MATERIAL PROPERTIES | 17 |
| II. TEST SUMMARY | 18 |
| III. MODEL DIMENSIONAL DATA | 19 |
| IV. DATA FOR MELT LINES PRESENTED IN FIGURES 3 THRU 8 | 20 |
| FIGURES | 21 |

INDEX OF MODEL FIGURES

| Figures | Title | Page |
|---------|--|------|
| 1. | Axis Systems | 21 |
| 2 | Model Sketches | |
| | a. Protuberance Model | 22 |
| | b. Nozzle Locations | 23 |
| 3. | Melt Lines at 20 Degrees Angle of Attack | 24 |
| | a. RCS Ports Closed $Re/ft = 10^6/ft, T_{pc} = 113^\circ F$ | |
| | b. RCS Ports Open $Re/ft = 10^6/ft, T_{pc} = 113^\circ F$ | |
| | c. RCS Ports Closed $Re/ft = 2 \times 10^6/ft, T_{pc} = 113^\circ F$ | |
| | d. RCS Ports Open $Re/ft = 2 \times 10^6/ft, T_{pc} = 113^\circ F$ | |
| 4. | Melt Lines at 25 Degrees Angle of Attack | 25 |
| | a. RCS Ports Closed $Re/ft = 10^6/ft, T_{pc} = 113^\circ F$ | |
| | b. RCS Ports Open $Re/ft = 10^6/ft, T_{pc} = 113^\circ F$ | |
| | c. RCS Ports Closed $Re/ft = 2 \times 10^6/ft, T_{pc} = 131^\circ F$ | |
| | d. RCS Ports Open $Re/ft = 2 \times 10^6/ft, T_{pc} = 131^\circ F$ | |
| 5. | Melt Lines at 30 Degrees Angle of Attack | 26 |
| | a. RCS Ports Closed $Re/ft = 10^6/ft, T_{pc} = 113^\circ F$ | |
| | b. RCS Ports Open $Re/ft = 10^6/ft, T_{pc} = 113^\circ F$ | |
| | c. RCS Ports Closed $Re/ft = 2 \times 10^6/ft, T_{pc} = 131^\circ F$ | |
| | d. RCS Ports Open $Re/ft = 2 \times 10^6/ft, T_{pc} = 131^\circ F$ | |
| 6 | Melt Lines at 35 Degrees Angle of Attack | 27 |
| | a. RCS Ports Closed $Re/ft = 10^6/ft, T_{pc} = 113^\circ F$ | |
| | b. RCS Ports Open $Re/ft = 10^6/ft, T_{pc} = 113^\circ F$ | |

INDEX OF MODEL FIGURES (Continued)

| Figures | Title | Page |
|---------|---|------|
| | c. RCS Ports Closed $Re/ft = 2 \times 10^6/ft$, $T_{pc} = 131^\circ F$ | |
| | d. RCS Ports Open $Re/ft = 2 \times 10^6/ft$, $T_{pc} = 131^\circ F$ | |
| 7 | Melt Lines at 40 Degrees Angle of Attack | 28 |
| | a. RCS Ports Closed $Re/ft = 10^6/ft$, $T_{pc} = 113^\circ F$ | |
| | b. RCS Ports Open $Re/ft = 10^6/ft$, $T_{pc} = 113^\circ F$ | |
| | c. RCS Ports Closed $Re/ft = 2 \times 10^6/ft$, $T_{pc} = 131^\circ F$ | |
| | d. RCS Ports Open $Re/ft = 2 \times 10^6/ft$, $T_{pc} = 131^\circ F$ | |
| 8. | Melt Lines at 45 Degrees Angle of Attack | 29 |
| | a. RCS Ports Closed $Re/ft = 10^6/ft$, $T_{pc} = 113^\circ F$ | |
| | b. RCS Ports Open $Re/ft = 10^6/ft$, $T_{pc} = 113^\circ F$ | |
| | c. RCS Ports Closed $Re/ft = 2 \times 10^6/ft$, $T_{pc} = 131^\circ F$ | |
| | d. RCS Ports Open $Re/ft = 2 \times 10^6/ft$, $T_{pc} = 131^\circ F$ | |

REPRODUCIBILITY OF THE
ORIGINAL PAGE IS POOR

NOMENCLATURE

| <u>SYMBOL</u> | <u>PLOT SYMBOL</u> | <u>DEFINITION</u> |
|---------------|-------------------------------------|---|
| C_p | C | specific heat of the model material - BTU/lb-°F |
| g | | acceleration due to gravity, 32.17 ft/sec ² |
| h | H(T ₀) | heat transfer coefficient based on T _{AW} = T ₀ |
| | H(.9T ₀) | heat transfer coefficient based on T _{AW} = 0.9 T ₀ |
| | H(r _{low} T ₀) | heat transfer coefficient based on T _{AW} = r _{low} x T ₀ |
| h_g | HREF | reference heat-transfer coefficient based on Fay-Riddell Theory, BTU/ft ² -sec.-°R |
| M_∞ | MACH NO. | free stream Mach no. |
| N_r | R | reference sphere radius used to calculate h_g (0.04 ft) |
| P_∞ | P-INF | free stream static pressure, psia |
| Pr | | Prandtl number |
| P_0 | PO | tunnel stilling chamber pressure, psia |
| P_1, P_2 | | defined in context |
| q_0 | Q-INF | free-stream dynamic pressure, psia |
| R | | universal gas constant, ft-lb _f /lb _m -°R |
| Re/ft | RE/FT | free stream unit Reynolds number, ft ⁻¹ |
| | ROLL-MODEL | model roll angle-deg. |
| ST | ST(T ₀) | Stanton number based on T ₀ : $ST(T_0) = \frac{H(T_0)}{p_\infty V_\infty [.2235 + 1.35 \times 10^{-4} (T_0 + 560)] \times 32.17}$ |
| r_{low} | | minimum recovery factor used in data reduction; function of angle of attack; r is non-dimensional |

NOMENCLATURE (Continued)

| <u>SYMBOL</u> | <u>PILOT SYMBOL</u> | <u>DEFINITION</u> |
|---------------|-------------------------|---|
| | STREF | reference Stanton number: $ST(TO) = \frac{HREF}{p_{\infty} V_{\infty} [.2235 + 1.35 \times 10^{-4} (T_o + 560)] \times 32.17}$ |
| T_{aw} | | adiabatic wall temperature, °F |
| \bar{T} | TBAR | $\frac{T_{pc} - T_{IN}}{T_{aw} - T_{IN}}$ |
| T_{IN} | | initial model temperature, °F |
| T_{∞} | T-INF | free stream static temperature-°R |
| T_{pc} | TPC | paint melt temperature, °F |
| T_o | TO | tunnel stilling chamber temperature, °R |
| t | TIME | time from start of model injection, sec. |
| Δt | DEL TIME | time model exposed to airstream, sec. |
| V_e | | velocity at edge of the boundary layer, ft/sec. |
| V_{∞} | V-INF | free stream velocity, ft/sec. |
| α | ALPHA-MODEL | model angle of attack, deg. |
| | ALPHA-PREBEND | sting prebend angle, deg. |
| | ALPHA-SECTOR | tunnel sector pitch angle-deg. |
| | YAW | model yaw angle |
| γ | | ratio of specific heats of air |
| k | K | model thermoconductivity, BTU/ft-sec-°F |
| β | | negative model yaw (positive sideslip) |

NOMENCLATURE (Concluded)

| <u>SYMBOL</u> | <u>PLOT SYMBOL</u> | <u>DEFINITION</u> |
|-----------------|------------------------|---|
| μ_{∞} | MU-INF | free stream viscosity, lb-sec/ft ² |
| μ_s | | stagnation air viscosity, lb-sec/ft ² |
| μ_w | | air viscosity along model wall (lb _m /ft-sec) |
| ρ | RHO | model material density-lb _m /ft ³ |
| ρ_w | | air density along model wall-lb _m /ft ³ |
| ρ_s | | stagnation air density lb _m /ft ³ |
| ρ_{∞} | RHO-INF | free stream air density, slug/ft ³ |

INTRODUCTION

Aerodynamic heating phase change paint tests were conducted on a .040 scale Rockwell International Space Shuttle Orbiter for 1. These tests were conducted in the AEDC VKF B Hypersonic Wind Tunnel Sept. 1, 1975.

The purpose of these tests was to determine the effects of simulated RCS nozzles, protuberances, and penetrations on aerodynamic heating rates during simulated entry conditions. The model was tested from 20° through 45° angle of attack at 0° and -1° angle of sideslip. All the above attitudes were tested at a nominal Mach number of 8. Reynolds number was varied from $0.5 \times 10^6/\text{ft}$ through $2.0 \times 10^6/\text{ft}$.

CONFIGURATIONS INVESTIGATED

The models were 0.040 scale representations of the forward 50% of the Rockwell International Space Shuttle Orbiter as defined by Rockwell lines VL70-000140C. The Rockwell model designation was 82-0. The models were cast in one piece using Lockheed proprietary material "LH" on a steel sting. There were no movable or removable model parts. Models used for this test were the 82-1 (paint stripe model) and 82-4 (protuberance model). The "smooth" model was the 82-4 with filled RCS nozzles and penetrations. Figures 2a and 2b illustrate the protuberances and penetrations simulated on the model.

REPRODUCIBILITY OF THE
ORIGINAL PAGE IS 100%

TEST FACILITY DESCRIPTION

The Arnold Engineering Development Center (AEDC) is an Air Force Facility located in Tullahoma, Tennessee. The tunnel used, Tunnel B, is located in the von Karman Facility portion of this center. Engineering and other technical operations in this tunnel are performed by contractor personnel of ARO, Inc.

Tunnel B is a continuous, closed circuit, variable density wind tunnel with an axisymmetric contoured nozzle and a 50-inch diameter test section. The tunnel can be operated at a nominal Mach number of 6 or 8 at stagnation pressures from 20 to 300 and 50 to 900 psia, respectively, and at a stagnation temperature of up to 1350°R. The model may be injected into the tunnel for a test run and then retracted for model cooling or model changes without interrupting the tunnel flow.

TEST PROCEDURE

Tempilaq[®], a fusible coating that changes phase from an opaque solid to a transparent liquid at temperatures specified by the manufacturer, was used to indicate the location of isotherms on the model surface. The paints used had melting temperatures of 113, 125, 131, 150, and 175 °F.

Beattie-Coleman Varitron[®] 70 mm sequence cameras were used to record the progression of isotherms on the windward surfaces, as a function of time, during each test run. The cameras were located on the top and side of the wind tunnel and photographed the left side and bottom surfaces of the orbiter models. The cameras were operated at a nominal rate of 1 frame/sec. Kodak TRI-X Pan[®] black-and-white film was used.

Dual television monitors were used throughout the test to facilitate on-line cross-referencing.

Prior to each test run, the model was cleaned with a solvent, spray-painted with the phase-change coating, and allowed to reach isothermal conditions. The model was then injected into the wind tunnel for about 30 seconds, during which time the progression of the isotherms, indicated by the demarcation between melted and unmelted coating, was continuously photographed. The model was then retracted from the wind tunnel and the cycle repeated for the next run. The model temperature was measured prior to each run using a thermocouple probe.

REPRODUCIBILITY OF THE
ORIGINAL PAGE IS GUARANTEED

TEST PROCEDURE (Continued)

The tests were conducted at the following nominal conditions:

| M_∞ | P_o, psia | $T_o, ^\circ\text{R}$ | $h_s \left[\frac{\text{BTU}}{\text{ft}^2 \cdot \text{sec} \cdot ^\circ\text{R}} \right]$ | $Re/ft \times 10^{-6}$ |
|------------|--------------------|-----------------------|---|------------------------|
| 7.90 | 110 | 1,270 | 0.0116 | 0.5 |
| 7.94 | 210 | 1,270 | 0.0162 | 1.0 |
| 7.98 | 430 | 1,300 | 0.0230 | 2.0 |

DATA REDUCTION

Thin film heat transfer coefficients were calculated for each melt line at which photographs were taken. The coefficients were calculated assuming three different recovery factors.

$$\frac{T_{aw}}{T_o} = r_{low}, 0.90, \text{ and } 1.0$$

The following calculations were then performed to obtain thin film coefficients:

$$\bar{T} = \frac{T_{pc} - T_{IN}}{T_{aw} - T_{IN}}$$

$$T_{aw} = \left(\frac{T_{aw}}{T_o} \right) \times T_o$$

$$h = \frac{\beta \sqrt{k \rho C_p}}{\sqrt{t}} \text{ AVG}$$

NOTE:

$$\sqrt{k \rho C_p} \text{ AVG} = \frac{\sqrt{k \rho C_p} \big|_{T_{IN}} + \sqrt{k \rho C_p} \big|_{T_{pc}}}{2}$$

where the flow parameter β results from iterative solution of:

$$1 - \bar{T} = e^{\beta^2} (1 - \text{erf } \beta)$$

Theoretical thin film heat transfer coefficients and stagnation point heating rates were calculated using the equations given below:

$$h_s = (.768)(C_p)(P_r)^{-0.6}(\rho_w \mu_w)^{.1}(\rho_s \mu_s)^{.4} \sqrt{\frac{dV_e}{dx}}$$

where

$$P_r = \frac{\mu C_p}{k} \text{ (}\mu, C_p \text{ and } k \text{ for air)}$$

$$\frac{dV_e}{dx} = \text{The streamwise velocity gradient along the model surface}$$

and

$$\frac{dV_e}{dx} = \frac{1}{N_r} \sqrt{2 R_g T_o \left(1 - \frac{1}{P_1 P_2} \right)}$$

$$N_r = \text{Nose radius, } 0.0175 \text{ foot radius (1 foot full scale)}$$

DATA REDUCTION (Concluded)

$$P_1 = \left[\frac{\gamma + 1}{2} M_\infty^2 \right]^{\frac{\gamma}{\gamma - 1}}$$

$$P_2 = \left[\frac{\gamma + 1}{2\gamma M_\infty^2 - (\gamma - 1)} \right]^{\frac{\gamma}{\gamma - 1}}$$

Melt lines are shown on selected photographs taken during the test and are presented at the back of this report. The melt line on each photograph shows isotherms. Thin film coefficients and free stream data corresponding to the isotherms are presented in Table IV. The photographs are presented to provide qualitative data showing effects of the protuberances and depressions.

RESULTS AND DISCUSSION

Uncertainties of the basic tunnel parameters were estimated from repeat calibrations of the PO and TO instruments and from the repeatability and uniformity of the tunnel flow during calibrations. The parameters PO, TO, and MACH NO. with their uncertainties were then used to compute the uncertainties in the other parameters dependent on these by means of the Taylor series method of error propagation.

| Uncertainty, percent | | | | |
|----------------------|-----------|-----------|--------------|-------------|
| <u>MACH NO.</u> | <u>PO</u> | <u>TO</u> | <u>RE/FT</u> | <u>HREF</u> |
| ± 0.4 | ± 0.1 | ± 0.4 | ± 1.2 | 0.8 |

An estimate of the data precision of phase change paint data is hampered by the fact that an observer must determine the location of the melt line. For this analysis, only uncertainties attributable to the measured parameters are considered. The parameters needed for the solution of the equation for the heat-transfer coefficient, h , are T_{pc} , T_{IN} , T_{aw} , $\sqrt{\rho k C_p}$, and Δt . The table below summarizes the nominal uncertainties in these specific parameters.

| <u>Parameter</u> | <u>Uncertainty (+)</u> |
|---------------------|------------------------|
| Δt | ± 1.0 |
| $\sqrt{\rho k C_p}$ | ± 10.0 |
| T_{IN} | ± 0.5 |
| $T_o (T_{aw})$ | ± 0.5 |
| T_{pc} | ± 0.5 |

RESULTS AND DISCUSSION (Concluded)

It should be remembered that the above uncertainties in T_{aw} and T_{pc} only reflect nominal measurement uncertainties. As previously mentioned, the interpretation of when phase change occurs (i.e., T_{pc}) is a matter of observer experience, and the "correct" assumption of what should be used for T_{aw} also requires engineering judgment. However, combining the above measurement uncertainties with the corresponding error sensitivity factor (derived by using the equation for the heat-transfer coefficient, h , and taking the square root of the sum of the squares) yields the following:

for $T_{pc} \leq 200^{\circ}\text{F}$, h uncertainty $\approx \pm 13$ percent

for $T_{pc} > 200^{\circ}\text{F}$, h uncertainty $\approx \pm 11$ percent.

REFERENCES

- 1) Test Data from the NASA/Rockwell International Space Shuttle Test (OH-75) conducted in the AEDC VKF Tunnel B, by L. Carter and C. Kaul.
- 2) Test Facilities Handbook (Tenth Edition). "von Karman Gas Dynamics Facility, Vol. 3." Arnold Engineering Development Center, May, 1974.
- 3) "Pretest Information for Phase Change Paint Tests on the 82- ϕ .040 Scale 50% Forebody Models of the Rockwell International Space Shuttle Orbiter in the AEDC VKF 'B' Hypersonic Wind Tunnel (OH-75)," SD-SH-0203, By W. H. Dye, dated August, 1975.

TABLE I
MODEL MATERIAL PROPERTIES

| <u>T_{pc}, °F</u> | <u>TEMPERATURE AT WHICH PROPERTIES WERE EVALUATED, °F</u> | <u>$\sqrt{\frac{\rho C k}{p}}$, Btu/ft²-°R-sec^{1/2}</u> |
|---------------------------|---|--|
| 113 | 95.5 | 0.0478 |
| 125 | 101.5 | 0.0481 |
| 131 | 104.5 | 0.0483 |
| 150 | 114.0 | 0.0487 |
| 175 | 125.5 | 0.0493 |

The model material properties were evaluated at a temperature equal to the average of the initial and phase-change paint temperatures.

TABLE II
TEST SUMMARY

| $\frac{Re}{ft}$ $\times 10^{-6}$ (ft-l) | MODEL ALPHA (deg) | YAW (deg) | PAINT MELT TEMP ($^{\circ}F$) | SMOOTH MODEL GROUP NO. | PROTUBERANCE MODEL GROUP NO. |
|---|-------------------------|--------------|---------------------------------------|------------------------------|------------------------------------|
| 0.5 | 30 | 0 | 113 | 42 | 39 |
| | 35 | 0 | 125 | 43 | 40 |
| | 35 | 1.0 | 125 | 44 | 41 |
| | 40 | 0 | 113 | 11 | 8 |
| | 40 | 1.0 | 113 | 10 | 9 |
| 1.0 | 20 | 0 | 131 | 34 | 27 |
| | 25 | 0 | 113 | 33 | 28 |
| | 30 | 0 | 113 | 32 | 29 |
| | 30 | 1.0 | 125 | 35 | 38 |
| | 35 | 0 | 113 | 31 | 30 |
| | 35 | 1.0 | 125 | 36 | 37 |
| | 40 | 0 | 113 | 12 | 4 |
| | 40 | 0 | 125 | -- | 6 |
| | 45 | 0 | 113 | 13 | 5 |
| | 45 | 0 | 125 | -- | 7 |
| 2.0 | 20 | 0 | 131 | 16 | -- |
| | 20 | 0 | 175 | 18 | 25 |
| | 25 | 0 | 131 | 19 | 22 |
| | 25 | 0 | 175 | 17 | -- |
| | 30 | 0 | 131 | 20 | 23 |
| | 35 | 0 | 131 | 21 | 26 |
| | 40 | 0 | 131 | 14 | 1 |
| | 45 | 0 | 131 | 15 | 2 |
| | 45 | 0 | 150 | -- | 3 |

Data Group 24 had no computer data. This group number was then voided.

REPRODUCIBILITY OF THE
TEST DATA IS 100%

①

TABLE III
MODEL DIMENSIONAL DATA

MODEL COMPONENT: BODY - B₆₀
 GENERAL DESCRIPTION: 50% orbiter forebody, vehicle 140C.
 NOTE: This body includes a small portion of the wing glove.

 MODEL SCALE: 0.040

 DRAWING NUMBER: VL70-000140C

| DIMENSIONS: | FULL SCALE | MODEL SCALE |
|-------------|---------------|--------------|
| Length | <u>645.15</u> | <u>25.80</u> |
| Max Width | <u>330.00</u> | <u>13.20</u> |

MODEL COMPONENT: CANOPY - C₁₀
 GENERAL DESCRIPTION: Configuration 4 canopy and windshield as
used with B₂₅, six glass panes in windshield

 MODEL SCALE: 0.040

 DRAWING NUMBER: VL70-000140B, 140C, 202B

| DIMENSIONS: | FULL SCALE | MODEL SCALE |
|---------------------------------------|-------------------|-------------------|
| Length ($X_0 = 434.643$ to 670) In. | <u>235.357</u> | <u>9.414</u> |
| Max Width | <u> </u> | <u> </u> |
| Max Depth Glass - In. | <u>28.00</u> | <u>1.12</u> |
| Nose/windshield intersection, $X_0 =$ | <u>434.643</u> | <u>17.386</u> |

TABLE IV DATA FOR MELT LINES PRESENTED IN FIGURES 3 THROUGH 8

| Figure | Group | α | Mach No. | Re/ft $\times 10^{-6}$ | P_0 (Psia) | T_0 (°R) | h_g ($H_f - 0.04$ ft.) | h/h_g | | | ST (τ_0) |
|--------|-------|----------|----------|---------------------------|-----------------|---------------|------------------------------|-----------|------------------|---------------------|--------------------|
| | | | | | | | | (T_0) | ($\cdot 9T_0$) | Flow ^{10*} | |
| 3a | 34 | 19.99 | 7.94 | 1.029 | 212.5 | 1269 | 0.01624 | 0.0498 | 0.0610 | 0.0688 | 0.001308 |
| 3b | 27 | 19.98 | 7.94 | 1.020 | 212.3 | 1275 | 0.01625 | 0.0503 | 0.0616 | 0.0694 | 0.001326 |
| 3c | 18 | 20.00 | 7.98 | 1.989 | 431.2 | 1299 | 0.0298 | 0.0856 | 0.1057 | 0.1199 | 0.001617 |
| 3d | 25 | 19.99 | 7.98 | 1.995 | 432.0 | 1298 | 0.0230 | 0.0864 | 0.1068 | 0.1210 | 0.001630 |
| 4a | 33 | 24.97 | 7.94 | 1.027 | 212.7 | 1271 | 0.01626 | 0.0239 | 0.0292 | 0.0329 | 0.000631 |
| 4b | 28 | 24.97 | 7.94 | 1.018 | 211.8 | 1275 | 0.01623 | 0.0239 | 0.0292 | 0.0328 | 0.000631 |
| 4c | 19 | 24.98 | 7.98 | 1.985 | 430.9 | 1300 | 0.02297 | 0.0474 | 0.0579 | 0.0650 | 0.000893 |
| 4d | 22 | 24.99 | 7.98 | 1.982 | 431.2 | 1302 | 0.02299 | 0.0493 | 0.0602 | 0.0676 | 0.000935 |
| 5a | 32 | 29.98 | 7.94 | 1.024 | 212.5 | 1273 | 0.01625 | 0.0256 | 0.0312 | 0.0351 | 0.000675 |
| 5b | 29 | 29.99 | 7.94 | 1.011 | 210.6 | 1276 | 0.01619 | 0.0257 | 0.0312 | 0.0351 | 0.000680 |
| 5c | 20 | 30.00 | 7.98 | 1.986 | 431.3 | 1300 | 0.02298 | 0.0273 | 0.0333 | 0.0374 | 0.000517 |
| 5d | 23 | 30.01 | 7.98 | 1.987 | 431.9 | 1301 | 0.02300 | 0.0277 | 0.0339 | 0.0380 | 0.000526 |
| 6a | 31 | 35.00 | 7.94 | 1.020 | 211.6 | 1273 | 0.01622 | 0.0246 | 0.0301 | 0.0338 | 0.000650 |
| 6b | 30 | 35.00 | 7.94 | 1.017 | 210.9 | 1272 | 0.01619 | 0.0252 | 0.0308 | 0.0345 | 0.000667 |
| 6c | 21 | 35.01 | 7.98 | 1.998 | 431.9 | 1297 | 0.02299 | 0.0260 | 0.0318 | 0.0358 | 0.000492 |
| 6d | 26 | 35.00 | 7.98 | 1.995 | 432.8 | 1300 | 0.02302 | 0.0259 | 0.0316 | 0.0355 | 0.000490 |
| 7a | 12 | 40.07 | 7.94 | 1.009 | 212.1 | 1294 | 0.01626 | 0.0197 | 0.0240 | 0.0270 | 0.000524 |
| 7b | 4 | 40.01 | 7.94 | 1.022 | 211.5 | 1296 | 0.01621 | 0.0197 | 0.0241 | 0.0270 | 0.000521 |
| 7c | 14 | 39.98 | 7.98 | 1.993 | 430.5 | 1296 | 0.02295 | 0.0232 | 0.0284 | 0.0319 | 0.000440 |
| 7d | 1 | 39.99 | 7.98 | 1.975 | 431.2 | 1305 | 0.02300 | 0.0241 | 0.0294 | 0.0331 | 0.000458 |
| 8a | 13 | 45.00 | 7.94 | 1.020 | 210.9 | 1270 | 0.01619 | 0.0450 | 0.0549 | 0.0616 | 0.001139 |
| 8b | 5 | 45.01 | 7.94 | 1.024 | 212.0 | 1271 | 0.01623 | 0.0461 | 0.0563 | 0.0632 | 0.001217 |
| 8c | 15 | 45.00 | 7.98 | 1.994 | 431.6 | 1297 | 0.02298 | 0.0438 | 0.0535 | 0.0602 | 0.000829 |
| 8d | 2 | 45.02 | 7.98 | 1.987 | 431.4 | 1300 | 0.0299 | 0.0467 | 0.0570 | 0.0641 | 0.000847 |

* $\frac{a}{\text{Flow}}$
 20 0.892
 25 0.902
 30 0.912
 35 0.923
 40 0.934
 45 0.945

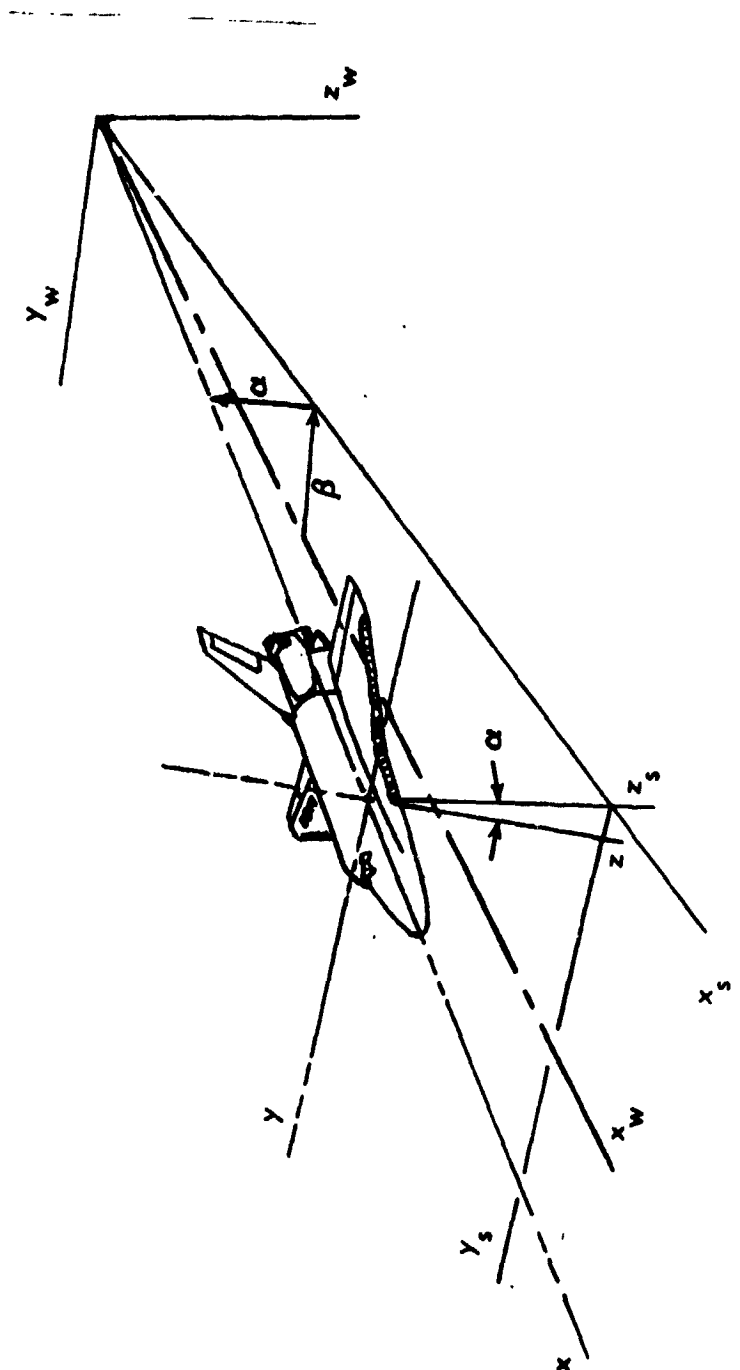
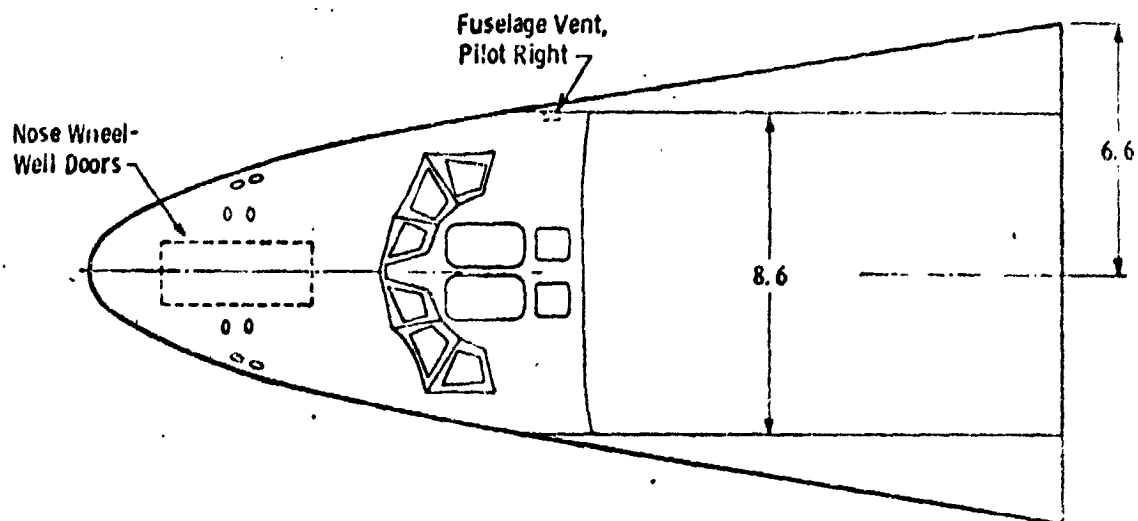
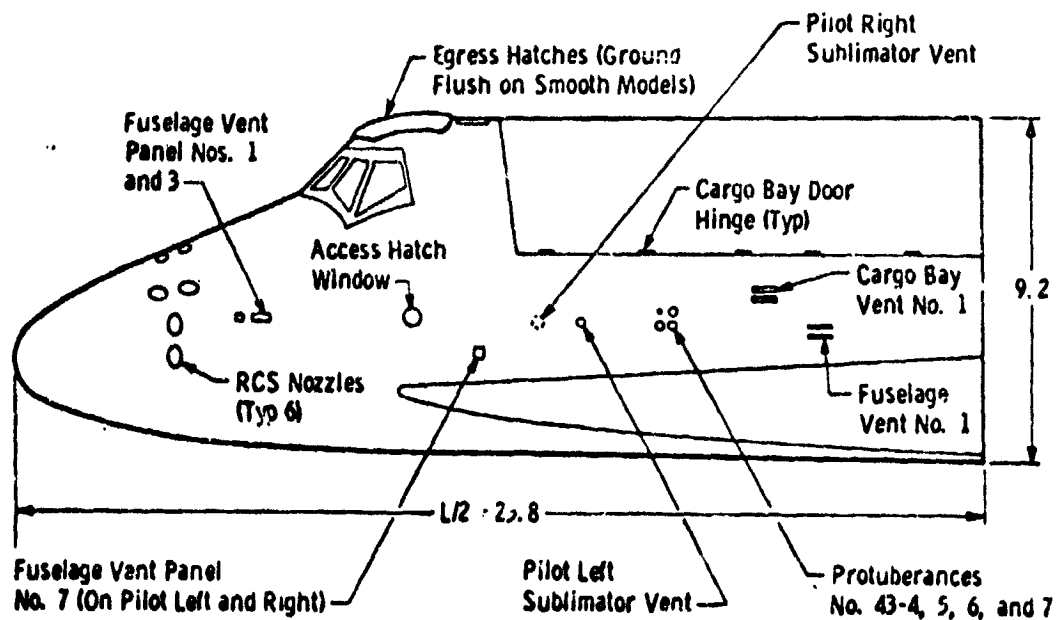


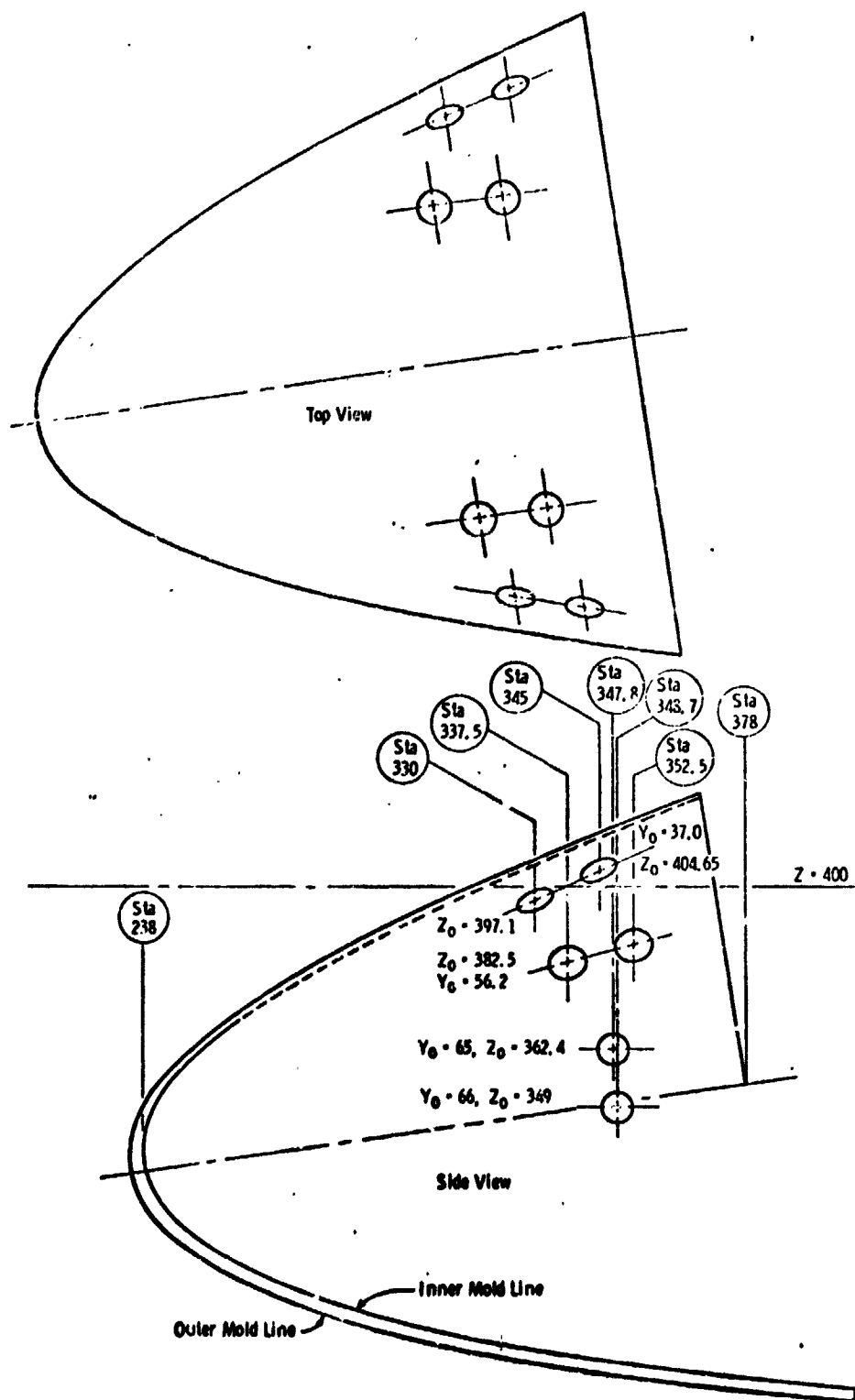
Figure 1. - Axis Systems.



Note: The smooth paint models had the same basic dimensions as are shown here but did not have the protuberances.
All dimensions are in inches.



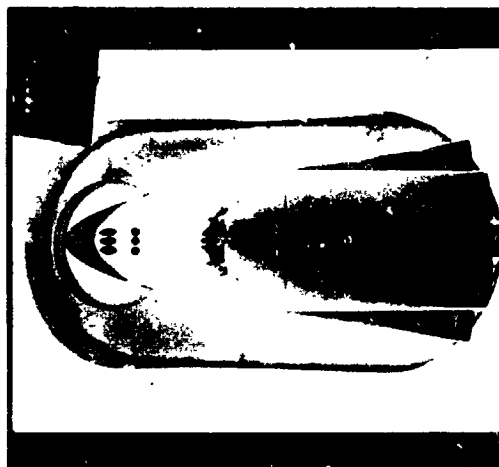
a. Protuberance Model
Figure 2. Model Sketches



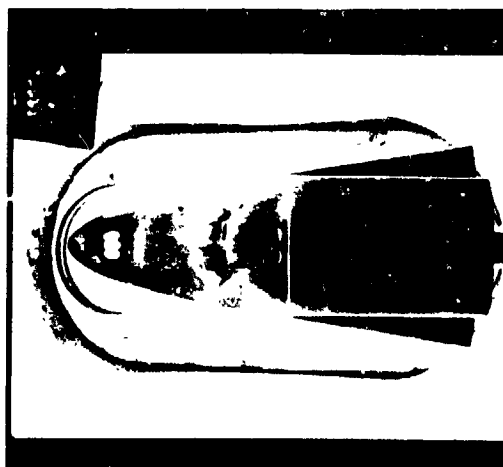
b. Nozzle Locations
Figure 2. (Continued)



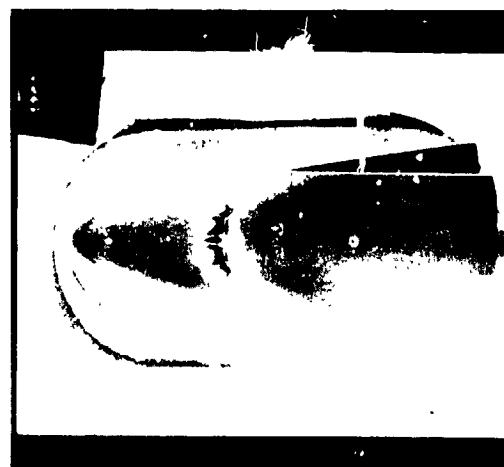
a. RCS Ports Closed
 $Re/ft = 10^6/ft$
 $T_{pc} = 113^{\circ}F$



b. RCS Ports Open
 $Re/ft = 10^6/ft$
 $T_{pc} = 113^{\circ}F$

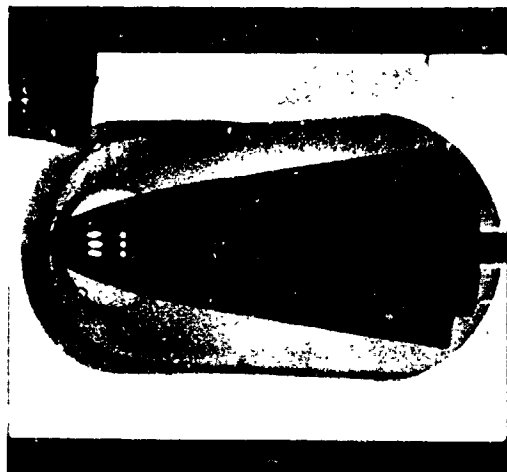


c. RCS Ports Closed
 $Re/ft = 2 \times 10^6/ft$
 $T_{pc} = 113^{\circ}F$

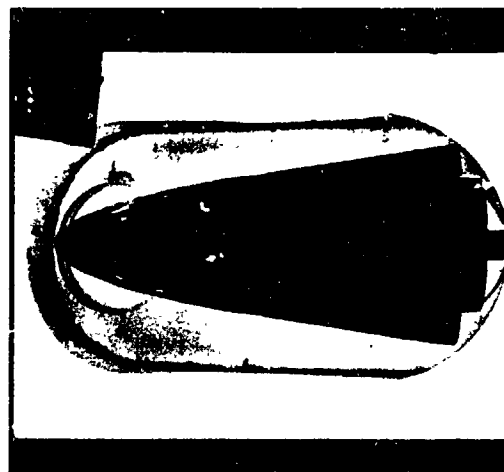


d. RCS Ports Open
 $Re/ft = 2 \times 10^6/ft$
 $T_{pc} = 113^{\circ}F$

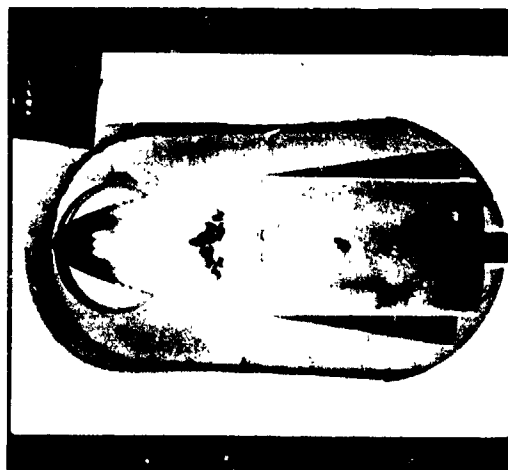
Figure 3. Melt Lines at 20 Degrees Angle of Attack



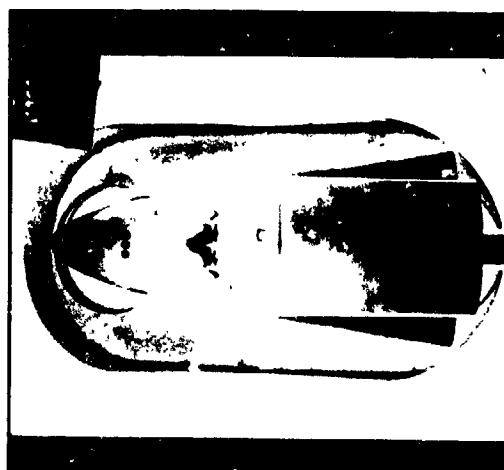
a. RCS Ports Closed
 $Re/ft = 10^6/ft$
 $T_{pc} = 113^{\circ}F$



b. RCS Ports Open
 $Re/ft = 10^6/ft$
 $T_{pc} = 113^{\circ}F$

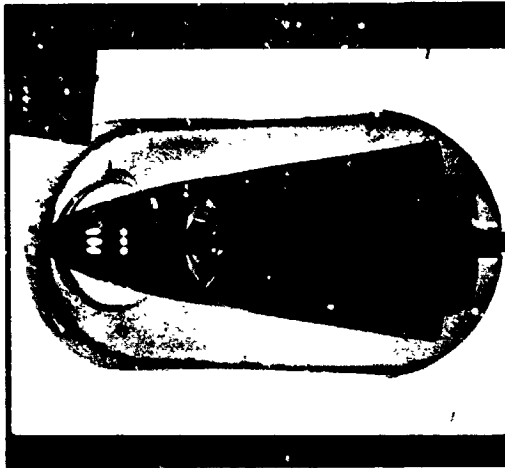


c. RCS Ports Closed
 $Re/ft = 2 \times 10^6/ft$
 $T_{pc} = 131^{\circ}F$

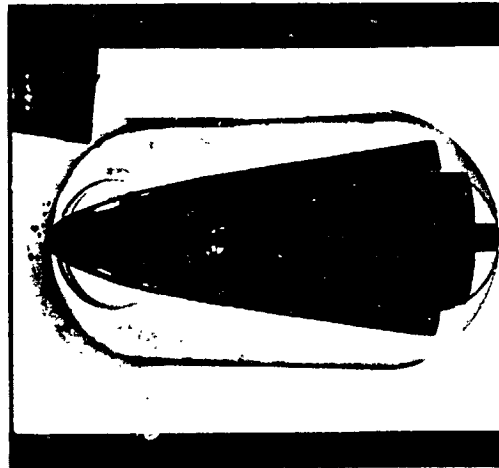


d. RCS Ports Open
 $Re/ft = 2 \times 10^6/ft$
 $T_{pc} = 131^{\circ}F$

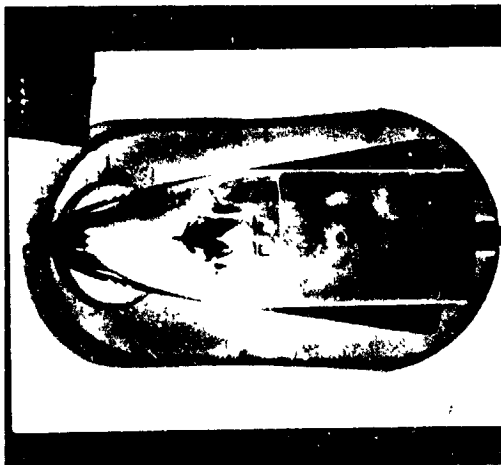
Figure 4. Melt Lines at 25 Degrees Angle of Attack



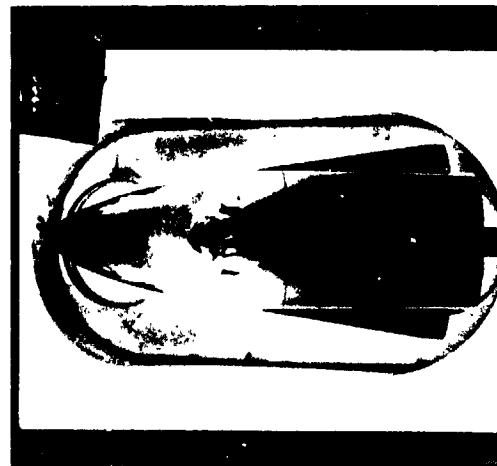
a. RCS Ports Closed
 $Re/ft = 10^6/ft$
 $T_{pc} = 113^{\circ}F$



b. RCS Ports Open
 $Re/ft = 10^6/ft$
 $T_{pc} = 113^{\circ}F$

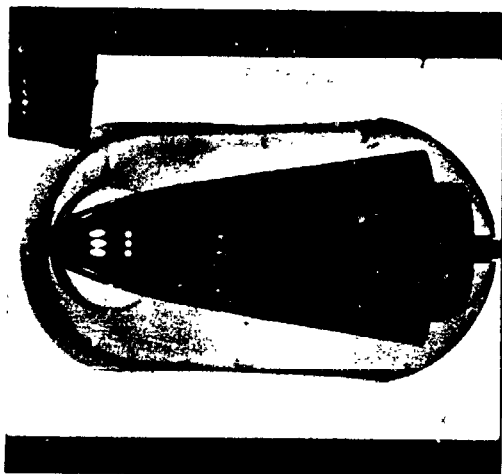


c. RCS Ports Closed
 $Re/ft = 2 \times 10^6/ft$
 $T_{pc} = 131^{\circ}F$

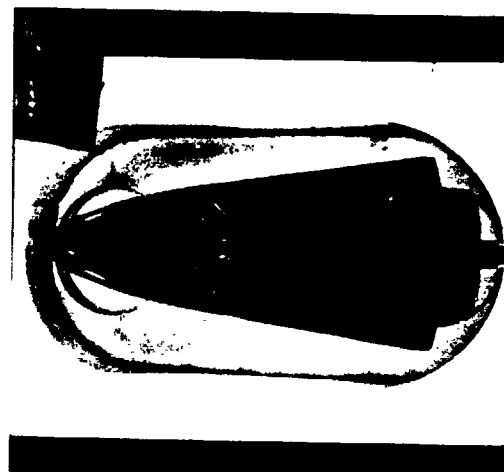


d. RCS Ports Open
 $Re/ft = 2 \times 10^6/ft$
 $T_{pc} = 131^{\circ}F$

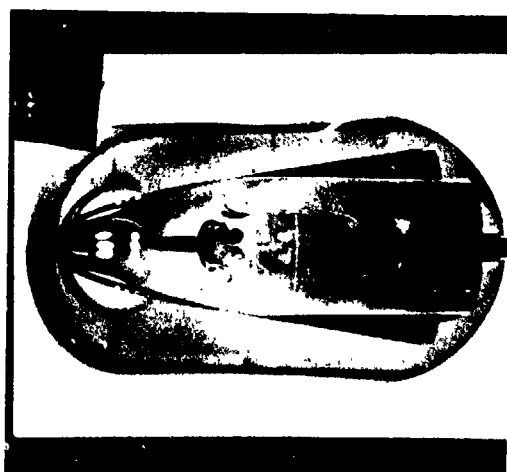
Figure 5. Melt Lines at 30 Degrees Angle of Attack



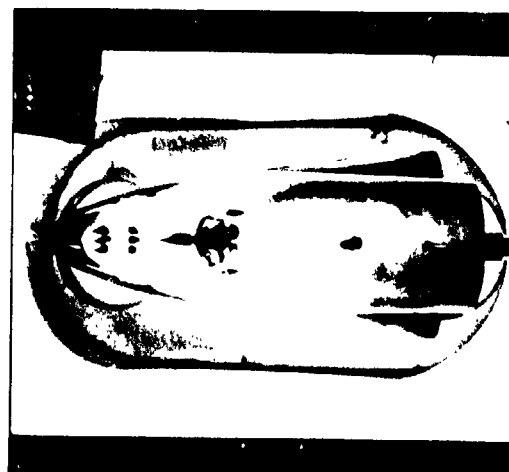
a. RCS Ports Closed
 $Re/ft = 10^6/ft$
 $T_{pc} = 113^\circ F$



b. RCS Ports Open
 $Re/ft = 10^6/ft$
 $T_{pc} = 113^\circ F$

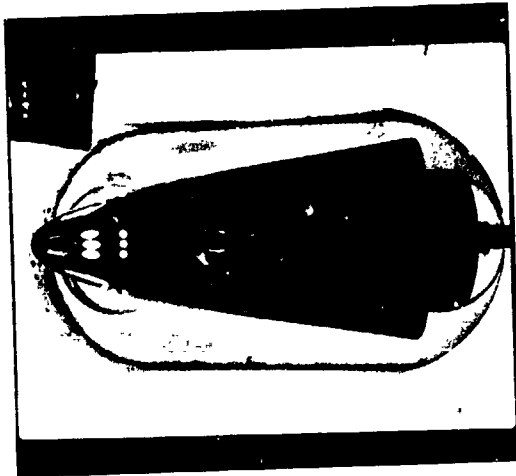


c. RCS Ports Closed
 $Re/ft = 2 \times 10^6/ft$
 $T_{pc} = 131^\circ F$

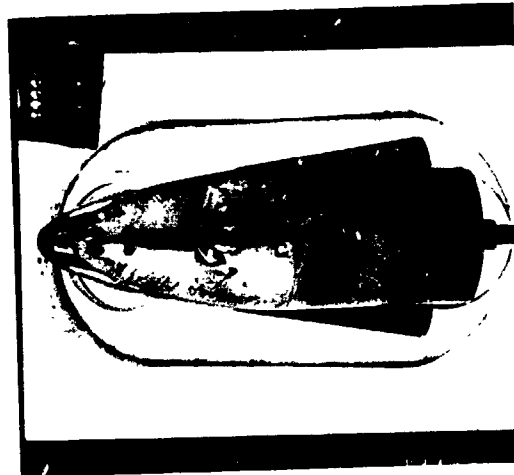


d. RCS Ports Open
 $Re/ft = 2 \times 10^6/ft$
 $T_{pc} = 131^\circ F$

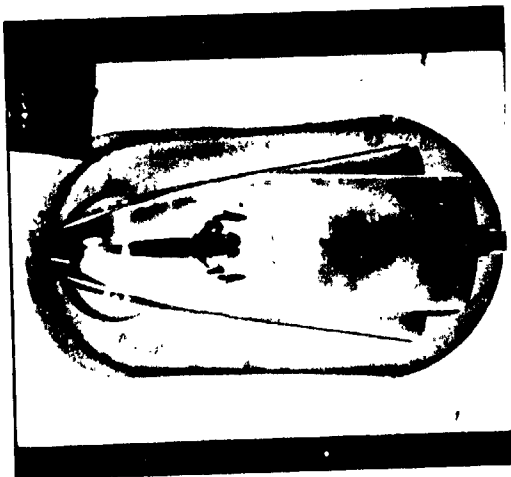
Figure 6. Melt Lines at 35 Degrees Angle of Attack



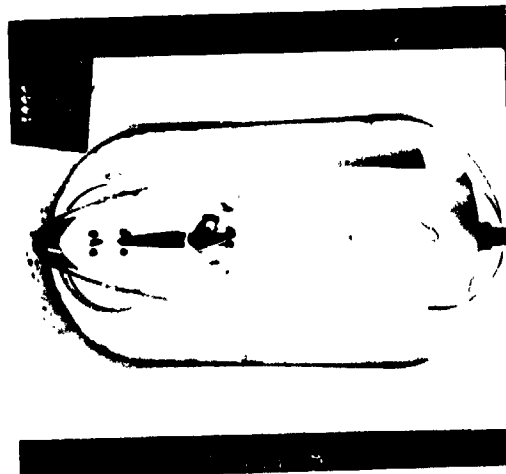
a. RCS Ports Closed
 $Re/ft = 10^6/ft$
 $T_{pc} = 113^{\circ}F$



b. RCS Ports Open
 $Re/ft = 10^6/ft$
 $T_{pc} = 113^{\circ}F$

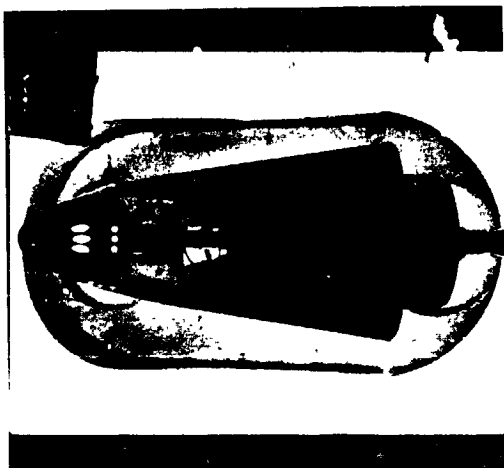


c. RCS Ports Closed
 $Re/ft = 2 \times 10^6/ft$
 $T_{pc} = 131^{\circ}F$

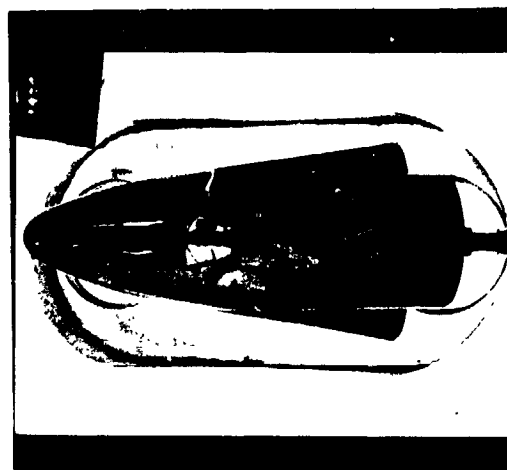


d. RCS Ports Open
 $Re/ft = 2 \times 10^6/ft$
 $T_{pc} = 131^{\circ}F$

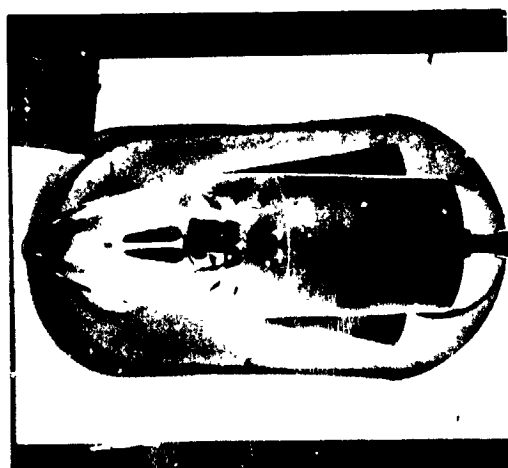
Figure 7. Melt Lines at 40 Degrees Angle of Attack



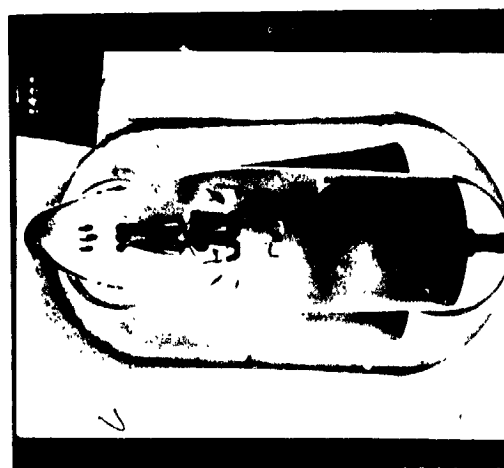
a. RCS Ports Closed
 $Re/ft = 10^6/ft$
 $T_{pc} = 113^\circ F$



b. RCS Ports Open
 $Re/ft = 10^6/ft$
 $T_{pc} = 113^\circ F$



c. RCS Ports Closed
 $Re/ft = 2 \times 10^6/ft$
 $T_{pc} = 131^\circ F$



d. RCS Ports Open
 $Re/ft = 2 \times 10^6/ft$
 $T_{pc} = 131^\circ F$

Figure 8. Melt Lines at 45 Degrees Angle of Attack